Letters in Applied NanoBioScience
Platinum Open Access Journal (ISSN: 2284-6808)

Article
Volume 9, Issue 3, 2020, 1225 – 1238
https://doi.org/10.33263/LIANBS93.12251238

Influence of Surface Charge on the Functional Properties of Silica Nanoparticles and Cellular Toxicity

L.A. Avinash Chunduri [1], K. Madhusudhana Rao [2], Vijaya Sai K. [3,*], Aditya D. Kurdekar [3], C. Prathibha [3], Venkataramaniah Kamisetti [1, 3,*]

[1] Grey Scientific Laboratories, Visakhapatnam, A.P., India
[2] Vignan's Institute of Information Technology, Visakhapatnam, A.P., India
[3] Laboratories for Nanoscience and Nanotechnology Research, Department of Physics, Sri Sathya Sai Institute of Higher Learning, Prasanthi Nilayam, A.P., India
* Correspondence: vrkamistti@gmail.com;

Scopus Author ID 13006925900
Received: 22.05.2020; Revised: 12.06.2020; Accepted: 14.06.2020; Published: 16.06.2020

Abstract: The effect of silica nanoparticles with a different surface charge on the cell viability of Caco-2 and RAW 264.7 cell lines was studied. Silica nanoparticles with narrow size distribution were prepared by Stobers method. These silica nanoparticles surface charge was varied from highly positive to highly negative, were single functionalized by APTES and multi functionalized by cysteine for amine and carboxyl groups. All other properties of the nanoparticles were kept constant. The unfunctionalized nanoparticles were used as control. Fourier Transform Infrared spectroscopy (FTIR) confirmed the presence of amine and carboxyl groups present on the surface of silica nanoparticles. The zeta potential measurements confirmed the successful modification of surface charge of silica nanoparticles in water. SEM images showed that the negatively charged, positively charged, and unfunctionalized nanoparticles with similar size and shape. MTT assay results indicated that the toxicity of SiO_2 was cell type-dependent. CaCo-2 cells were highly resistant to nanoparticle treatment whereas RAW 264.7 (macrophages) predominantly charge dependent. The difference in toxicity could be attributed to the difference in the physiological function of each cell line. Among the three kinds of nanoparticles (negative, positive, and untreated), positively charged nanoparticles showed higher toxicity, which might be due to the attractive interaction between the negatively charged cell membrane and positively charged SiO_2 nanoparticles.

Keywords: SiO_2 nanoparticles; Surface charge; Cytotoxicity; Caco-2 cells; RAW cells; MTT assay.

1. Introduction

Nanotechnology involves the creation and manipulation of materials at nanoscale levels to create products that exhibit novel properties. There are important applications of nanoscience in biology and biotechnology, and nanotechnology offers new tools to biologists 1-6]. Nevertheless, despite the increased interest in the development of nanoparticles, few studies address their potential toxicity. The rapidly developing field of nanotechnology is likely to become yet another source of human exposure to nanoparticles by different routes: inhalation, ingestion, dermal, and injection. Regulatory agencies, researchers, and health and environmental watchdogs are assessing how nanoscale materials affect human health and environment [7]. Similarly, the characteristic biokinetic behavior of nanoparticles is an attractive quality for promising applications in medicine. Such applications include diagnostic

and therapeutic devices and tools to investigate and understand molecular processes and structures in living cells. However, in stark contrast to the many efforts aimed at exploiting the desirable properties of nanoparticles for improving human health, attempts to evaluate potential undesirable effects when administered for medical purposes or after exposure during manufacture or processing for industrial applications are limited.

Nanotoxicology, an emerging discipline, is gaining increased attention. Nanotoxicology research will not only provide data for safety evaluation of engineered nanostructures and devices but will also help to advance the field of nanomedicine by providing information about their undesirable properties and means to avoid them [7]. The safety and toxicity of nanoparticles are of growing concern despite their significant scientific interest and promising potential in many applications. Their biological activity and biokinetics are dependent on many parameters: size, shape, chemistry, charge, surface modifications, etc. When inhaled, they can translocate out of the respiratory tract via different pathways and mechanisms. When ingested, systemic uptake of nanoparticles via lymph can occur. When in blood circulation, they can distribute throughout the organism, and they are taken up by liver, spleen, bone marrow, heart, and other organs such as testis. The study of the toxic effect of nanoparticles on gametogenesis is of great interest. The identification of toxic properties of new compounds at an early stage has a high priority before human or animal testing in vivo can begin.

Despite many established bioconjugation strategies for targeting purposes with silica NPs, concerns regarding their clinical success have risen. Recently, it has been shown that the targeting capability and stability of bioconjugated NPs may disappear when they are placed in a biological environment. The primary reason is the presence of a complex mixture of distinct proteins in the biological media. Prior to cellular uptake, these proteins adsorb rapidly onto the surface of NPs, leading to the formation of a so-called “corona”, which may obscure specific recognition of bioligands on the NPs surface and hamper their targeting applicability. Indeed, at physiological conditions, biological systems are often exposed to NP-protein corona complexes, which differ significantly from bare NPs and define surface properties, aggregation rate, and hydrodynamic size of NPs{8,9].

The purpose of this study is to assess how surface functional groups on silica NPs can be exploited to control cell responses. In this study, we report the synthesis of silica NPs, which was followed by introducing amino and carboxyl groups at carefully chosen concentrations to generate single- or multi functionalized silica NPs. Thereby, the surface charge was tuned successfully over a broad range from highly positive to highly negative, whereas other properties such as size, morphology, and hydrophilicity remained approximately constant. This strategy enabled us to separate the effect of the net surface charge from the effects of the other mentioned physicochemical properties and to solely investigate the influence of surface charge on the interactions of the silica NPs with proteins and cells, without interference by other factors [10]. The synthesized silica nanoparticles were characterized by scanning electron microscopy (SEM), Fourier transform infrared spectroscopy (FTIR), zeta potential, and dynamic light scattering (DLS).

2. Materials and Methods

2.1. Cell culture requirements.

2.1.1 Biosafety cabinet.

All the cell culture experiments need to be performed in a biosafety cabinet (also called cell culture hood). It is designed to protect the experimentalist from any infectious contaminations arising from experimental splashes and mishandlings or from aerosols produced by the microbial processes. It also prevents the contamination of the cell culture from human interactions. The laminar airflow in the hoods protects the culture and keeps the work environment from dust and other airborne contaminants with its unidirectional flow of filtered air. The workspace in the cell culture hood is to be maintained clean and uncluttered and arranged neatly in a direct line of sight. Animal cell culture is generally done in biosafety level II cabinets. BSL-2 is suitable for the culture and maintenance of medium-risk cell lines. Apart from the biosafety cabinets, personal protective equipment (PPE) like gloves, lab coats, footwear, safety lab glasses, etc. are a must while handing biohazardous materials and cell lines [11]. All the cell culture reported in this thesis were performed in a BSL-2 cabinet under expert supervision.

2.1.2 CO_2 incubator.

The healthy growth and multiplication of cells require that the temperature, moisture, and air mixture is maintained at appropriate levels (typically, 37, 5% CO2, or mammalian cells). A CO2 incubator maintains the aforementioned optimal conditions required for the growth and development of cells. Apart from that, it should also maintain aseptic conditions to prevent contamination of the cells.

2.1.3. Cell growth medium.

Besides the conditions of temperature and gas mixture, the most pertinent factor in cell culture systems is the cell growth medium. Minimal Essential Medium (MEM) is a cell culture medium developed by Harry Eagle and is used to maintain cells. It contains amino acids, essential salt, glucose, and vitamins. • Dulbecco's modified Eagle's medium (DMEM), contains approximately four times as much of the vitamins and amino acids present in MEM and two to four times as much glucose. Additionally, it also contains iron. Additionally, a serum-supplement like a fetal bovine serum (FBS) or other serum growth factors are used to supplement the culture media for the in vitro cell culture of eukaryotic cells8.

2.1.4. Caco-2 cell line.

The Caco-2 cells are epithelial-like continuous cell lines from human epithelial colorectal adenocarcinoma cells, originally developed by the Sloan-Kettering Institute for Cancer Research by Dr. Jorgen Fogh [12]. These are heterogenous adherent cell lines derived from the human large intestine or colon carcinoma. On culturing under specific conditions, these cells differentiate and get polarized in a manner that their phenotype bears a resemblance to that of the enterocytes of the small intestine [13,14]. Caco-2 cells express tight junctions, microvilli, and a number of enzymes and transporters that are specific of enterocytes: peptidases, esterases, P-glycoprotein, uptake transporters for amino acids, bile acids carboxylic

acids, etc. Caco-2 cells are most commonly used not as individual cells, but as a confluent monolayer on a cell culture insert filter. When cultured in this format, the cells differentiate to form a polarized epithelial cell monolayer that provides a physical and biochemical barrier to the passage of ions and small molecules. The Caco-2 monolayer is widely used across the pharmaceutical industry as an in vitro model of the human small intestinal mucosa to predict the absorption of orally administered drugs [15]. The correlation between the in vitro apparent permeability across Caco-2 monolayers and the in vivo fraction absorbed is well established. The Caco-2 cell culture model is not only a rapid screening tool for drug absorption studies but, for this study, is a tool to measure mucosal toxicity caused by excipients such that their influence on membrane barrier properties and, ultimately, the mechanism of drug absorption can be understood [16].

2.1.5. Caco-2 culture and cytotoxicity conditions and protocol.

Culture medium: Eagle's Minimum Essential Medium (pH 7.4)

• Other additives: Heat inactivated fetal bovine serum (Gibco, Invitrogen), sodium bicarbonate, antimycotic and antibacterial mixture, and gentamycin
• Passage number: 12 – 25
• Period of cell culture: 20 days
• Number of replicates: 3
• Test compound concentration: 50µg/mL - 1000µg/mL
• Incubation time: 24 hours
• Temperature: 37
• Assay type: Cell viability, MTT assay
• Compound requirements: 100 µL of 10 mM DMSO solution
• Analysis method: SpectraMax M 5, Molecular devices quantification Cell culture

The cell culture experiments were performed in a biosafety level II cabinet hood. The Caco-2 cells of passage number 12-25 were cultured using the minimum essential medium, MEM (pH 7.4), in culture plates at 37 in a CO_2 incubator. The other supplements added to the medium were heat-inactivated fetal bovine serum, sodium bicarbonate, antimycotic and antibacterial mixture, and gentamycin. The medium was changed every alternate day until the cells became 80% confluent. The washing of the cells was done using phosphate buffer saline, and the removal of cells was performed by trypsinization (0.25% trypsin,0.2% EDTA solution) at 37 for 7-10 minutes. The cells obtained from trypsinization were obtained as a pellet by centrifugation for 3 minutes at 200 x g and resuspended into the MEM and used for sub-culturing or cytotoxicity studies.

2.1.6. RAW 264.7 cells.

RAW 264.7 cells are a macrophage-like, Abelson leukemia virus-transformed cell line derived from BALB/c mice. This cell line is a commonly used model of mouse macrophages for the study of cellular responses to microbes and their products. RAW-Blue™ cells express the secreted alkaline phosphatase (SEAP) reporter gene. A model macrophage commonly used to represent the physiological scavengers of foreign nanoparticles exposed to *in vivo* systems.

2.1.7. Culture of RAW cells - cytotoxicity conditions and protocol.

• Culture medium: ATCC-formulated Dulbecco's Modified Eagle's Medium, (pH7.2)
• Other additives: Foetal bovine serum (Gibco, Invitrogen), 2 mM Glutamine
• Passage number: 8 – 15
• Period of cell culture: 15 days
• Number of replicates: 3
• Test compound concentration: 50µg/mL - 1000µg/mL
• Incubation time: 24 hours
• Temperature: 37
• Assay type: Cell viability, MTT assay
• Compound requirements: 100 µL of 10 mM DMSO solution
• Analysis method: SpectraMax M 5, Molecular devices quantification
• culture conditions: air, 95%; carbon dioxide (CO2), 5% and 37

Split sub-confluent cultures (70-80%) 1:2 to 1:8 i.e. seeding at 2-4x10,000 cells/cm²; 5% CO2; 37°C. Use cell scrapers to remove the attached cells. Cells are semi-adherent, i.e., some cells grow in suspension, some loosely attach to the surface, and others flattened out and attached to the flask. Cells should not be allowed to overgrow and become confluent as this can lead to loss of the flattened adherent cell characteristic. Cells will pinocytose neutral red and phagocytose zymosan. Cells capable of antibody-dependent lysis of sheep erythrocytes and tumor targets. Growth inhibited by LPS.

2.1.8. MTT assay.

Cell-based assays are often used for screening collections of compounds to determine if the test molecules have effects on cell proliferation or show direct cytotoxic effects that eventually lead to cell death. These assays are also useful for measuring receptor binding and a variety of signal transduction events that may involve the expression of genetic reporters, trafficking of cellular components, or monitoring organelle function. Regardless of the type of cell-based assay being used, it is important to know how many viable cells are remaining at the end of the experiment.

There are a variety of assay methods that can be used to estimate the number of viable eukaryotic cells. The MTT assay is a colorimetric cell viability assay used for assessing cell metabolic activity. It is based on enzymes called the NAD(P)H-dependent cellular oxidoreductase. These enzymes have the capacity to reduce the tetrazolium dye, MTT or 3-(4,5- dimethylthiazol-2-yl)-2,5-diphenyltetrazolium bromide which is a pale yellow colored tetrazole, to its insoluble formazan, which is purple in color. The reduction of this tetrazolium dye would depend upon the amount of NAD(P)H-dependent oxidoreductase enzymes that are present predominantly in the cytosolic compartment of the cell.

This, in turn, is governed by the cellular metabolic activity due to NAD(P)H flux. Cells with low metabolism rates (such as thymocytes and splenocytes) would be able to reduce very little MTT. On the contrary, rapidly dividing cells can be expected to exhibit higher rates of MTT reduction due to the presence of a higher amount of the enzymes.

MTT reagent preparation: Dissolve MTT in Dulbecco's Phosphate Buffered Saline, pH=7.4 (DPBS) to 5 mg/ml. Filter-sterilize the MTT solution through a 0.2 µM filter into a sterile, lightly protected container. Store the MTT solution, protected from light, at 4 for frequent use, or at -20 for long term storage.

MTT assay protocol:

• Seed cells ~4,000/well and incubate for 48 hours.
• Prepare cells and test compounds in 96-well plates containing a final volume of 100 µl/well.
• Incubate for a desired period of exposure.
• Add 10 µL MTT Solution per well to achieve a final concentration of 0.45 mg/ml.
• Incubate for 2 hours at 37°C.
• Add 100 µL Solubilization solution to each well to dissolve formazan crystals.
• Mix to ensure complete solubilization.
• Record absorbance at 570 nm.

A solubilization solution (usually either dimethyl sulfoxide) is added to dissolve this insoluble purple-colored formazan product formed into a colored solution. The absorbance of this colored solution is quantified spectrophotometrically by measuring at a suitable wavelength (usually between 500 and 600 nm). The resuspended cells of Caco-2 cells obtained after trypsin treatment of an 80% confluent plate were seeded at a cell density of 4x103 in a 96 well plate for 48 hours and successively exposed to different concentrations of various nanoparticles made by the culture medium. The culture medium was changed after 48 hours of incubation, and the test solutions were added. For RAW cells, there is no trypsinization required. Since these are semi adherent, all the cells are collected via aspiration from the culture plate. After removing the old medium, all the cells were resuspended in fresh DMEM medium. Approximately 8,000 cells per well were added and incubated for 24 hours. After which for both the cell lines medium was removed and the test solutions (50-1000 µg/mL) were added to each well, and the plates were kept in CO_2 incubator for 24 hours. The cytotoxicity was assessed from the cell viability data obtained from the MTT [(3-(4,5-dimethylthiazol-2-yl)-2,5-diphenyltetrazonium bromide] cell proliferation assay.

After 48 hours of incubation, 20 µL of the MTT reagent was added to each well. The plates were then incubated for another 4 hours. Then the medium was removed and the intracellular formazan was solubilized with 100 mL of dimethyl sulfoxide (DMSO). The absorbance was recorded using a microplate reader (Spectramax M5) at 490 nm. Cell viability was assessed as the percentage of absorbance of the analyte with respect to the control. The data are presented as the mean standard error of the mean for the indicated number of separate experiments.

2.2. Synthesis of silica nanoparticles.

In a typical synthesis, Eu^{3+} doped silica nanoparticles (SiO_2:Eu NPs) were prepared using the modified Stoeber method [17]. To a mixture containing 4 mL of tetraethoxysilane (TEOS) and 47 mL of ethanol, 3.3 mL of ammonium hydroxide was added drop by drop along with vigorous stirring. ~~was~~. The stirring was continued for 24 hours resulting in a turbid solution. The solution was filtered, and the remaining solids were washed with ultrapure water and ethanol several times. These solid particles were dried under vacuum overnight at 80°C. Then these dried silica nanoparticles were used for the characterization and cytotoxicity studies.

2.3. Synthesis of Amine functionalized SiO_2:NH_2 NPs.

Amine functionalized silica nanoparticles (SiO_2–NH_2) were prepared by a silanization process with APTES [18]. Amine functionalization was conducted by stirring 300 mg of silica nanoparticles dispersed in 75 mL of ethanol with 83.75 microliters of APTES added drop by drop at room temperature. The reaction was continued overnight with stirring. The suspension was filtered, and the remaining solid nanoparticles were washed with water and ethanol for 3 times. These solid nanoparticles were subjected to vacuum drying at 60 ^oC.

2.4. Synthesis of cysteine functionalized SiO_2:NH_2 NPs.

We synthesized multi-functionalized silica nanoparticles by introducing both amine (-NH_2) and carboxyl (-COOH) groups onto their surface in a single step by cysteine. In a typical synthesis, cysteine molecules were immobilized by dispersing 30 mg of SiO_2 nanoparticles with 15 mg of cysteine in 30 mL of water. The reaction was continued for 2 hours with vigorous stirring. The mixture was washed 3 times with double distilled water and dried under vacuum at 60 °C. The successful functionalization of cysteine was confirmed by using thermogravimetric analysis and Fourier infrared spectroscopy. These multi-functionalized silica nanoparticles are abbreviated as SiO_2˙cys for further usage in the text.

2.5. Characterization of functionalized SiO_2 nanoparticles.

Characterization studies were performed for annealed and functionalized silica nanoparticle samples only.

2.5.1. FESEM analysis.

For FESEM analysis, SiO_2, SiO_2-NH_2 and SiO_2-cys were first dispersed in alcohol, and the dispersion was sonicated for 30 minutes before drop-casting. In the next step, these sonicated nanoparticles were drop cast on a silicon wafer (substrate) and dried under vacuum overnight. Since silica nanoparticles are non-conducting, we have gold coated the sample for a very short time (approx. 30-40 sec) before going for SEM imaging. Morphology and size were investigated by Field Emission Scanning Electron Microscope (FESEM), Zeiss Gemini Ultra 55, operated at 5 kV.

2.5.2. Fourier Transform Infrared (FTIR) analysis.

The presence of groups on the surface of silica nanoparticles post functionalization was confirmed using Fourier Transform Infrared (FTIR) spectroscopy. All FTIR spectra were collected using SHIMADZU IR Affinity-1, in the wavenumber range of 400-4000 cm-1 by KBr method in transmission mode with an accumulation of 32-time scans.

2.5.3. DLS analysis.

To measure the particle size and zeta potential, all three samples were dispersed in double-distilled water. All the measurements were done on dynamic light scattering equipment supplied by Malverin (Model: Zeta Sizer). All the measurements were done in triplicates for both the particle size analysis and zeta potential. The polydispersity index was (PDI) was calculated based on the cumulative analysis of the light scattering data, which was

automatically performed by the DLS instrument. The average sizes and standard deviations of data were obtained from three independent measurements.

2.6. Cytotoxicity studies.

Both Raw 264.7 and Caco-2 cells were seeded at a cell density of 2 X 10^3 and 4 X 10^3 cells, respectively, in 96 well plates for the cytotoxicity studies using MTT assay. The Raw cells were incubated for 24 hours, whereas Caco-2 cells were incubated for 48 hours before exposing them to nanoparticles in 5% CO_2 incubator at 37 ^oC. SiO_2, $SiO_2 – NH_2$, and $SiO_2 –$ COOH nanoparticles were suspended in culture media with varying concentrations of 50 – 1250 µg/mL were exposed to both the cell lines. The cytotoxicity was assessed by MTT cell proliferation assay. After 24 hours of incubation, the medium containing nanoparticles was removed, and the cells were washed with phosphate buffer saline. Then MTT solution was added to each well and incubated at 37^{o}C for in 5% CO_2 incubator for 2 hours. Next, 100 µL of DMSO (solubilizing solution) was added to each well, and the contents of each well were mixed gently. The OD (absorbance) of each well was measured using a microplate reader at 490 nm ((SpectraMax M5, Molecular Devices, USA). Cell viability was assessed as the percentage of absorbance of the analyte with respect to the control. The statistical significance of the difference with respect to control was investigated by the two-tailed Student's t-test.

3. Results and Discussion

FESEM analysis of SiO_2:Eu nanoparticles confirmed the size of all these nanoparticles to be between 50-70 nm (Figures 1, 2, 3). The carboxyl, thiol, and amino functional groups present on silica nanoparticles could influence short-range particle interactions. These induced agglomerations due to the intermolecular interaction caused mainly by hydrogen bonding among cysteine molecules. Even after functionalization, no size difference was observed in SiO_2-NH_2 and SiO_2-cys samples. All the images displayed are not to the scale. This confirmed uniform size of the silica nanoparticles from SEM images is very important to eliminate the influence of particle size on the cytotoxicity of Caco-2 and RAW cell lines that are chosen in this study. Figure 1a shows the FESEM image of silica nanoparticles (SiO_2) and Figure 1b and 1c shows the FESEM image of amine and carboxyl functionalized (SiO_2-cys) silica nanoparticles.

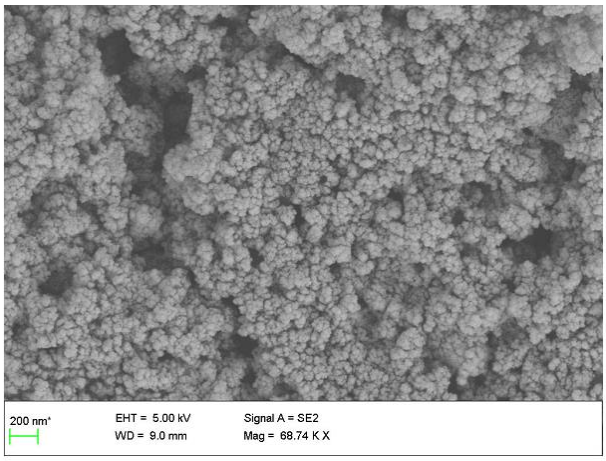

Figure 1. FESEM image of silica nanoparticles (SiO_2).

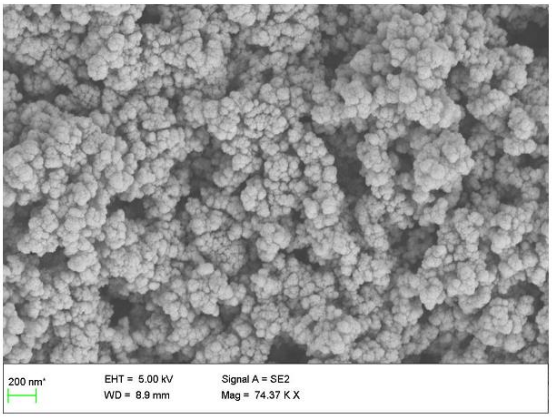

Figure 2. FESEM image of amine functionalized (SiO_2-NH_2) silica nanoparticles.

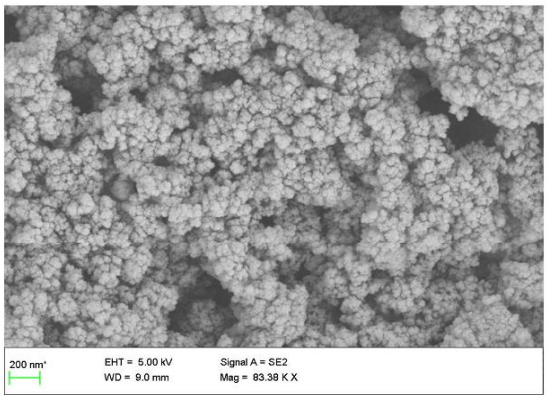

Figure 3. FESEM image of carboxyl functionalized (SiO_2-cys) silica nanoparticles.

Figure 2 shows the FTIR spectra of SiO_2, SiO_2-NH_2, and SiO_2-cys functionalized nanoparticles. The bands absorption peak at 1092 and 1220 cm^{-1} corresponds to the asymmetric and symmetric stretching vibrations of the Si-O-Si, which were observed in all the three samples. The band at 800 cm^{-1} indicates the presence of Si-OH stretching vibrations [19]. The band at 3150 cm^{-1} is attributed to the N-H stretching vibrations, which is present in the samples of amine and cysteine functionalized silica nanoparticles. The broadband at 3350 cm^{-1} can be ascribed to the characteristic absorption bands of the -OH stretching vibration mode. The appearance of bands at 1606 and 1107 cm^{-1} observed in the carboxyl functionalized sample supports that –COOH groups were present in the sample of cysteine functionalized SiO_2 nanoparticles [20].

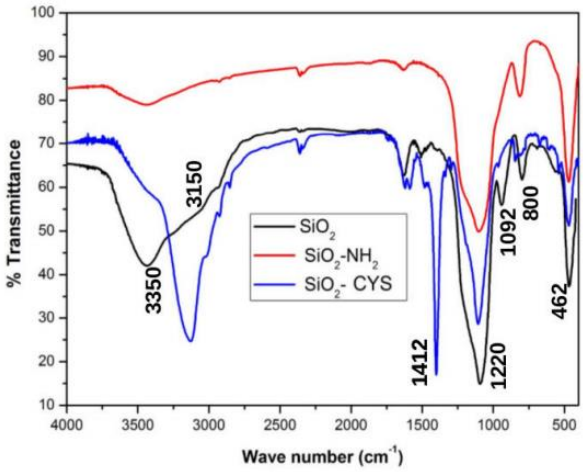

Figure 4. FTIR spectra of SiO_2, SiO_2-NH_2, and SiO_2-cys functionalized nanoparticles.

Table 1. DLS analysis of SiO_2, SiO_2-NH_2, SiO_2-cys for size, and zeta potential measurements.

Material	Size from FESEM (nm)	Size from DLS (nm)	PDI	Zeta Potential (mV)
SiO_2	80	124	0.366	-19.3 ± 1.7
SiO_2-NH_2	93	186	0.285	32.5 ± 2.2
SiO_2-cys	88	159	0.294	-26.6 ± 3.5

The nanoparticle diameter obtained from SEM images, the mean hydrodynamic particle sizes by DLS, PDI, and zeta potential values are summarized in Table 1. DLS measurements confirmed low PDI for all the three varieties of SiO_2 nanoparticles. From table 1, it can be seen that there is a slight increase in the particle sizes obtained by DLS when compared to FESEM. The largest particle size was observed for amine-functionalized nanoparticles which would be due to the electrostatic interactions between the amine functional groups. Cysteine functionalized silica could maintain its size to a good extent maybe because of the carboxyl groups present on the surface along with the amine groups. It is also clear that by changing the functionalities (intention is to change the surface charge), there is also change in the size which is only due to the interaction between the functional groups. This size difference would not affect our cytotoxicity tests because silica nanoparticle sizes above 50 nm did not exhibit any cytotoxicity, and it is very clear from the literature. Zeta potential measurement was used to confirm whether the proposed modifications can generate different surface charged silica nanoparticles. It can be observed from table 1 as expected that the silica nanoparticles modified with APTES (positively charged silica) have a zeta potential of 32.5 ± 2.2 mV in double-distilled water. This higher positive potential is because of the huge amount of amine groups present on the surface of the silica. The bare SiO_2 nanoparticles and SiO_2-NH_2 and SiO_2-COOH nanoparticles modified with cysteine (negatively charged) have negative potentials, and their values are -19.3 ± 1.7 and -26.6 ± 3.5 respectively. The negative potential is because of the hydroxyl and carboxyl groups present on their surface of these nanoparticles.

Caco-2 cell lines are often used as models to establish the membrane permeability of drugs. Silica nanoparticles have extensive applications in drug delivery, so we evaluated the different surface charges silica functionalized with different groups were studied for their cytotoxicity. RAW 264.7 cell line is very sensitive to small perturbations in the environment surrounding it. With small changes like pH and temperature also, the cells get activated and give raise to lobed morphology instead of spherical morphology.

RAW 264.7 is also a cancerous cell line, so the cell line was chosen to study the use of charged nanoparticles for cancer therapy applications. In order to evaluate comparative account on the cytotoxicity profiles of SiO_2, SiO_2-NH_2 and SiO_2-cys nanoparticles were exposed to Caco-2 and RAW264.7 cells with different concentrations for 24 hours. The cell viability was accessed using MTT assay. The concentration of the nanoparticles tested for cytotoxicity is in the range of 50 - 1250 µg/mL for both the cell lines.

The MTT assay results for Caco-2 cells (figure 5) show that there were almost no significant differences between the lowest concentration and also the highest concentration i.e. 1250 µg/mL of all the samples. But between the samples, non-functionalized SiO_2 has shown higher viability when compared to both the functionalized samples. SiO_2-NH_2 and SiO_2-cys nanoparticles both have exhibited almost the same percentage of viability except for 250 µg/mL. It was also observed that exposing cells to silica nanoparticles has stimulated cell growth. This phenomenon can be explained by a required induction period for the Caco-2 cell lines to adapt to the treatment with silica nanoparticles before proliferation. After the induction period, MTT assay results showed that exposing cells to silica nanoparticles substantially stimulated cell growth.

Most of the previous studies suggested that for silica nanoparticles, either the charge or the size above 50 nm did not show any signs of toxicity on Caco-2 cells. In summary, the MTT results in figure 5 also demonstrated that 50 µg/mL has the highest viability for all the three samples, and the concentration 1000, 1250 µg/mL, also proliferated well. This proves that all three varieties of silica nanoparticles are biocompatible. From this, it is very clear that the silica nanoparticles with varieties of functional groups don't induce any cytotoxicity for Caco-2 cells. The highest positive and negative charges could not induce any change in cell proliferation is an encouraging sign that these nanoparticles can be successfully employed for targeted drug delivery which requires the presence of $–NH_2$ and - COOH groups for linking specific groups to reach the site of interest.

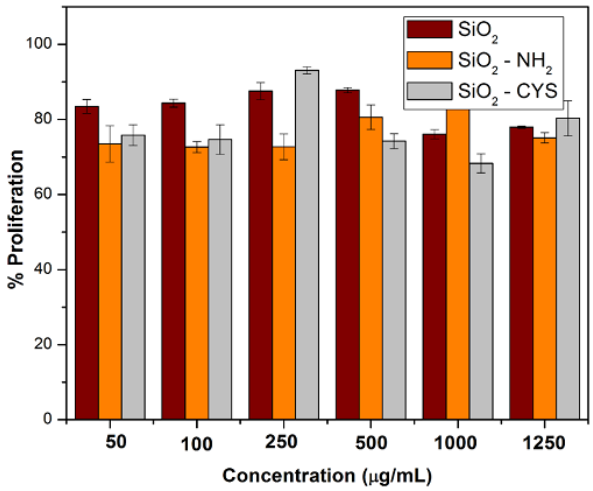

Figure 5. Viability of Caco-2 cell line on different dosages of SiO2, SiO2-NH2 and SiO2-cys by MTT assay. The polystyrene well without nanoparticles was used as the control. Data are presented as the average± SD for n = 5.

Figure 5~~3~~shows the viability of Caco-2 cell line on different dosages of SiO_2, SiO_2-NH_2, and SiO_2-cys by MTT assay. The polystyrene well without nanoparticles was used as the control. Data are presented as the average ± SD for n = 5. The ability of SiO_2 with the engineered chemical features and surface charges to induce acute cellular toxicity response was tested on RAW 264.7 and by MTT assay. Results demonstrated that the toxicity of SiO_2, SiO_2-NH2, and SiO_2-cys was highly cell type and nanoparticle concentration-dependent (figure 6). Both SiO_2 and SiO_2-cys at concentrations as high as 1000 µg/mL did not affect the relative viability of RAW 264.7 cells after 24 h exposure. But above this concentration, they exhibited a considerable amount of toxicity. But for all the concentrations, the positively charged silica (SiO_2-NH_2) caused dramatic toxicity leaving only 50-60% of the viable cells compared with controls even with 24 h treatment. The higher toxicity caused by SiO_2-NH_2 could be due to the presence of positive charge present on the surface. This is attributed to the higher penetration caused by the interaction between the negatively charged cell membrane and positively charged SiO_2-NH_2 nanoparticles. But for SiO_2 and SiO_2- cys, the presence of the negative charge on their surface did not affect the viability of the raw cells even at higher concentrations because of the repulsive forces between the negatively charged on the cell surface and the negatively charged nanoparticles. These results clearly demonstrate apart from the size, the charge of the nanoparticles also plays a greater role in cytotoxicity. So, in summary, these negatively charged SiO_2 and SiO_2- cys (contains both $–NH_2$ and -COOH groups) are nontoxic to RAW 264.7 cells. These results can provide useful guidelines for the rational design of SiO_2 in nanomedicine.

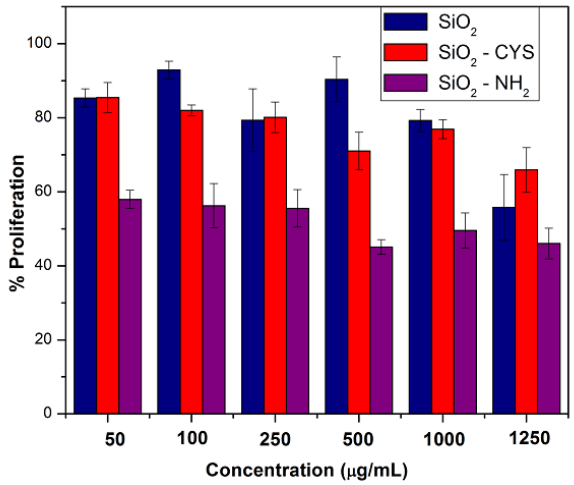

Figure 6. Viability of RAW 264.7 line on different dosages of SiO2, SiO2-NH2and SiO2-cys by MTT assay. The polystyrene well without nanoparticles was used as the control. Data are presented as the average ± SD for n = 5.

But for all the concentrations, the positively charged silica (SiO_2-NH_2) caused dramatic Figure 6: Viability of RAW 264.7 line on different dosages of SiO_2, SiO_2-NH_2, and SiO_2-cys by MTT assay. The polystyrene well without nanoparticles was used as the control. Data are presented as the average± SD for n = 5 toxicity leaving only 50-60% of the viable cells compared with controls even with 24 h treatment. The higher toxicity caused by SiO_2-NH_2 could be due to the presence of positive charge present on the surface. This is attributed to the higher penetration caused by the interaction between the negatively charged cell membrane and positively charged SiO_2-NH_2 nanoparticles. But for SiO_2 and SiO_2-cys the presence of the negative charge on their surface did not affect the viability of the raw cells even at higher concentration because of the repulsive forces between the negatively charged on the cell surface and the negatively charged nanoparticles. These results clearly demonstrate apart from the size the charge of the nanoparticles also plays a greater role in cytotoxicity. So, in summary, these negatively charged SiO_2 and SiO_2-cys (contains both –NH_2 and -COOH groups) are nontoxic to RAW 264.7 cells. These results can provide useful guidelines for the rational design of SiO_2 in nanomedicine.

4. Conclusions

The effect of silica nanoparticles with a different surface charge on the cell viability of Caco-2 and RAW 264.7 cell lines was studied. Silica Nanoparticles with narrow size distribution were prepared by Stoeber's method. These silica nanoparticles surface charge was varied from highly positive to highly negative, were single functionalized by APTES and multi-functionalized by cysteine for amine and carboxyl groups. All other properties of the nanoparticles were kept constant. The non-functionalized nanoparticles were used as control. Fourier Transform Infrared spectroscopy (FTIR) confirmed the presence of amine and carboxyl groups present on the surface of silica nanoparticles. The DLS measurements of SiO_2, SiO_2 - NH_2, and SiO_2-cys showed that particles zeta potential to be -19.3 ± 1.7, 32.5 ± 2.2 mV, and -26.6 ± 3.5 respectively. FESEM images confirmed that there is not much size variation in the particle sizes. The zeta potential measurements confirmed the successful modification of surface charge of silica nanoparticles in water. SEM images showed that the negatively charged, positively charged, and non-functionalized nanoparticles with similar size and shape. For Caco-2 cells, all silica nanoparticles have not exhibited any toxicity even with the highest

concentration of 1250 µg/mL. Our MTT assay results for Caco-2 cells suggested that the charge on the nanoparticles does not have any influence on the viability of these cells. The silica nanoparticles (SiO_2-NH_2) with positive charge could be more easily uptaken by the RAW 264.7 cell lines than other silica nanoparticles of similar size due to the attractive interaction between positively charged amine-functionalized nanoparticles and the negative cell membrane. The negatively charged silica nanoparticles have better biocompatibility compared to the SiO_2-NH_2 nanoparticles based on MTT assay for RAW cells. MTT assay results indicated that the toxicity of SiO_2 was cell type-dependent. CaCo-2 cells were highly resistant to nanoparticle treatment whereas RAW 264.7 (macrophages) predominantly charged dependent. The difference in toxicity could be attributed to the difference in the physiological function of each cell line. Among the three kinds of nanoparticles (negative, positive, and untreated), positively charged nanoparticles showed higher toxicity, which might be due to the attractive interaction between the negatively charged cell membrane and positively charged SiO_2 nanoparticles. These results provide an improved understanding of the influence of surface charge on functional properties of silica nanoparticles for various biomedical applications, especially for gene delivery and intracellular drug delivery fields.

Funding

This research received no external funding.

Acknowledgments

The authors are grateful to Bhagawan Sri Sathya Sai Baba for His constant guidance and support. We thankfully acknowledge the ORISE program fellowship awarded to L.A.A.C for training at CBER/FDA. We also thank the UGC, Govt. of India, for BSR fellowship to L.A.A.C.

Conflicts of Interest

The authors declare no conflict of interest.

References

1. Whitesides, G.M. The 'right' size in nanobiotechnology. *Nature Biotechnology* **2003**, *21*, 1161-1165, https://doi.org/10.1038/nbt872.
2. Bruchez M, Moronne M, Gin P, Weiss S, Alivisatos AP. Semiconductor nanocrystals as fluorescent biological labels. Science. **1998**, 281, 2013–2016.https://doi.org/10.1126/science.281.5385.2013
3. Chan WCW, Nie SM. Quantum dot bioconjugates for ultrasensitive nonisotopic detection. Science. **1998**,281, 2016–2018. http://doi.org/10.1126/science.281.5385.2016
4. Wang S, Mamedova N, Kotov NA, Chen W, Studer J. Antigen/antibody immunocomplex from CdTe nanoparticle bioconjugates. Nano Letters. **2002**, 2, 817–822.https://doi.org/10.1021/nl0255193
5. Mah C, Zolotukhin I, Fraites TJ, Dobson J, Batich C, Byrne BJ. Microsphere-mediated delivery of recombinant AAV vectors in vitro and in vivo. Mol Therapy. **2000**, 1, S239. https://doi.org/10.1006/mthe.2000.0174
6. Panatarotto D, Prtidos CD, Hoebeke J, Brown F, Kramer E, Briand JP, Muller S, Prato M, Bianco A. Immunization with peptide-functionalized carbon nanotubes enhances virus-specific neutralizing antibody responses. Chemistry&Biology. **2003**,10, 961–966. https://doi.org/10.1016/j.chembiol.2003.09.011
7. Oberdörster, G.; Oberdörster, E.; Oberdörster, J. Nanotoxicology: An Emerging Discipline Evolving from Studies of Ultrafine Particles. *Environmental Health Perspectives* **2005**, *113*, 823-839, https://doi.org/10.1289/ehp.7339.
8. Norrby, E. & Prusiner, S. B. Polio and nobel prizes: Looking back 50 years. Ann. Neurol.**2007**, 61, 385–395 https://doi.org/10.1002/ana.21153

9. Arathoon, W. R. & Birch, J. R. Large- Scale Cell Culture in Biotechnology. Science.**1986**, 232,1390–1395 https://doi.org/10.1126/science.2424083
10. Johnson, S., Nguyen, V. & Coder, D. Assessment of cell viability. Curr. Protoc. Cytom. **2013**. https://doi.org/10.1002/0471142956.cy0902s64
11. Hinrichs, T., Gragert, S. & Klein, M. Biological Safety Cabinets: Simulation and Quantifying of Airflow Perturbation Caused by Personnel Activities. Appl. Biosaf. **2016**, 1–7 http://doi.org/10.1177/1535676016661769
12. Fogh, J.; Fogh, J.M.; Orfeo, T. One Hundred and Twenty-Seven Cultured Human Tumor Cell Lines Producing Tumors in Nude Mice23. *JNCI: Journal of the National Cancer Institute* **1977**, *59*, 221-226, https://doi.org/10.1093/jnci/59.1.221.
13. Sambuy, Y.; De Angelis, I.; Ranaldi, G.; Scarino, M.L.; Stammati, A.; Zucco, F. The Caco-2 cell line as a model of the intestinal barrier: influence of cell and culture-related factors on Caco-2 cell functional characteristics. *Cell Biology and Toxicology* **2005**, *21*, 1-26, https://doi.org/10.1007/s10565-005-0085-6.
14. Alshehri, A.A. PhD thesis, University of Nottingham **2013**.
15. Shah, P., Jogani, V., Bagchi, T. & Misra, A. Role of Caco-2 cell monolayers in prediction of intestinal drug absorption. Biotechnol. Prog. **2006**, 22, 186–198 http://doi.org/10.1021/bp050208u
16. Artursson, P.; Borchardt, R.T. Intestinal Drug Absorption and Metabolism in Cell Cultures: Caco-2 and Beyond. *Pharmaceutical Research* **1997**, *14*, 1655-1658, https://doi.org/10.1023/A:1012155124489.
17. Francesco, E.; Raffaele, R.; Alvise, P.; Pietro, R.; Alvise, B. Synthesis and characterization of monodisperse Eu-doped luminescent silica nanospheres for biological applications *Proc. SPIE* **2008,** *6991*, 69912E–69912E–8, https://doi.org/10.1117/12.781504.
18. Labéguerie-Egéa, J.; McEvoy, H.M.; McDonagh, C. Synthesis, characterisation and functionalisation of luminescent silica nanoparticles. *Journal of Nanoparticle Research* **2011**, *13*, 6455-6465, https://doi.org/10.1007/s11051-011-0539-0.
19. Tagaya, M.; Ikoma, T.; Yoshioka, T.; Motozuka, S.; Xu, Z.; Minami, F.; Tanaka, J. Synthesis and luminescence properties of Eu(III)-doped nanoporous silica spheres. *Journal of Colloid and Interface Science* **2011**, *363*, 456-464, https://doi.org/10.1016/j.jcis.2011.07.066.